Excitability of excitons and biexcitons in a ring cavity

V. Z. Tronciu* and R. A. Abram
Department of Physics, University of Durham, Durham, DH1 3LE, United Kingdom
(Received 16 May 2001; revised manuscript received 23 October 2001; published 25 January 2002)

We discuss the excitable behavior of excitons and biexcitons in a nonlinear optical ring cavity. The nonlinearity is due to the process of the creation of biexcitons by photon-assisted conversion of excitons. In the bifurcation analysis a region where a saddle point is close to an equilibrium has been found. In this region the system shows excitability. It is shown that the mechanism of the excitable behavior of excitons and biexcitons in a ring cavity is different from that of two-level atoms in the same system. The possible applications of an excitable ring cavity are discussed.

DOI: 10.1103/PhysRevE.65.026616 PACS number(s): 05.45.Yv, 42.65.Sf

I. INTRODUCTION

Excitability is quite an old concept, which is particularly well known in biology [1–3] where it is used to explain a number of phenomena including neural communication by nerve cells via electrical signalling. A system is said to be excitable if a stimulus below some threshold value produces a negligible response while one above the threshold results in a substantial response which is essentially independent of the size of the stimulus. Excitability also occurs in chemistry [4], physics, and engineering [5–8]. Some general concepts of excitability in optics and associated models have been discussed in Ref. [9]. Excitability in optics is of great interest because of its prospects for applications in optoelectronics devices, primarily for optical switching, clock recovery, pulse reshaping, tuneable pulses, and for generating a coherent resonance output pulse in communication networks.

Reference [5] has proposed and discussed excitability in a ring cavity containing a homogeneously broadened two-level nonlinear medium. Excitability in this system occurs in the small parameter window close to a bistable operating region, and originates from the combined dynamical effects of nonlinear intracavity field saturation and temperature-dependent absorption in the medium on two different times scales. The origin of the excitability is similar to that in the FitzHugh-Nagumo model. More recently, excitability has been predicted in lasers with a saturable absorber [6], with delayed optical feedback [7] and with an integrated dispersive reflector [8]. In Ref. [6] it is shown that a laser with a saturable absorber displays excitability just below threshold. The analytical expression for the excitability threshold was obtained by considering the slow-fast nature of the system. Under the influence of optical noise the laser displays coherence resonance. Excitability in this system is due to an attractor close to a saddle point. This is the second type of mechanism leading to excitability that is found in literature.

In this paper, we have studied the excitability of excitons and biexcitons in a nonlinear optical ring cavity. The optical nonlinearity is considered to be due to the creation of biexcitons by the interaction of excitons and photons. The relaxation times of excitons and biexcitons are very short, being of the order of picoseconds, which means that mechanisms based on them are suitable for use in optoelectronic devices where ultrafast response is required. Biexcitons can be readily created in wide gap semiconductors such as CuCl, CuBr, and CdS where the electron-hole interaction is strong. But different mechanisms for their formation in bulk semiconductors have been proposed in the literature. The giant oscillator strength model which has been proposed by Hanamura, and Gogolin and Rashba [10,11] has been successfully applied to explain many biexciton-related optical processes in bulk semiconductors. More recently, Ivanov, Haug, and Keldysh have proposed a bipolariton model of biexcitons [12]. It has been shown [13–15] that both microscopic models can be used to form the basis of theoretical description of the phenomena of optical bistability, self pulsation, and chaos. Comparison with high-precision experiments supports the view [12,16] that the bipolariton model gives the better description of the microscopic processes, particularly in low-dimensional systems. Nevertheless, the giant oscillator model has had considerable success in bulk semiconductors and provides a basis for a model of excitability which is substantially more tractable than what is currently possible with the bipolariton theory.

The paper is structured as follow. In Sec. II we present the model equations for excitons, biexcitons, and photons in the ring cavity and the bifurcation analysis. Section III demonstrates excitable behavior in the system and the possible applications of excitability are discussed. The conclusions are given in Sec. IV.

II. DYNAMICS

A. Equations

For simplicity we use the three-level model which has been previously applied to a CuCl crystal, where there is convincing experimental evidence of the existence of biexcitons. In a CuCl crystal the biexciton bond energy is of the order of 40 meV and the exciton absorption band and the *M* band of biexciton recombination are well separated from each other. We study the simultaneous action of two independent optical pulses. The photons of the first pulse with energy $h\omega_1 = E_g - I_{ex}$ are in resonance with a transition in the exciton spectral range. The photons of the second pulse, which

*Author to whom correspondence should be addressed. Email address: V.Z.Tronciu@durham.ac.uk

cause exciton-biexciton conversion, have an energy $h\omega_2 = E_g - I_{ex} - I_{biex}$ and are in resonance with the region of the fluorescence M band of a CuCl crystal. E_g is the band gap, I_{ex} and I_{biex} are the exciton and biexciton binding energies, respectively.

The full Hamiltonian of the system consists of a sum of the Hamiltonians for free excitons, biexcitons, and the electromagnetic field, and the interaction Hamiltonian, which has the form

$$H_{int} = -\hbar g(aE_1^+ - a^\dagger E_1) - \hbar g G(a^\dagger E_2 b - a b^\dagger E_2^+),$$

where $a^\dagger$ and $b^\dagger$ are the creation operators of an exciton and a biexciton, respectively, and E_j^+ is the positive frequency component of the electric field of electromagnetic wave of the jth pulse ($j=1,2$). g is the constant of the exciton-photon interaction and G is the exciton-biexciton conversion coefficient. This Hamiltonian treats excitons and biexcitons as independent Bose quasiparticles.

The macroscopic equations for the positive-frequency field components E_j^+ and for the exciton (A) and biexciton (B) amplitudes [17], neglecting spatial dispersion have the form

$$c_1^2 \frac{\partial^2 E_1^+}{\partial z^2} - \frac{\partial^2 E_1^+}{\partial t^2} = 4\pi\hbar g \frac{\partial^2 A}{\partial t^2}, \tag{1}$$

$$c_2^2 \frac{\partial^2 E_2^+}{\partial z^2} - \frac{\partial^2 E_2^+}{\partial t^2} = 4\pi\hbar g G \frac{\partial^2 (A^* B)}{\partial t^2}, \tag{2}$$

$$i\frac{dA}{dt} = \omega_{ex} A - g E_1^+ - g G B E_1 - i\gamma_{ex} A, \tag{3}$$

$$i\frac{dB}{dt} = \omega_{biex} B - g G E_2^+ A - i\gamma_{biex} B, \tag{4}$$

where c_j is the velocity of jth field propagation in the medium, $\hbar\omega_{ex}$ ($\hbar\omega_{biex}$) is the energy of exciton (biexciton) formation and γ_{ex} and γ_{biex} are the inverse coherence lifetimes of excitons and biexcitons, respectively. Although the lifetimes can be considered as phenomenological parameters, Eqs. (3) and (4) can by derived rigorously using the quantum theory of fluctuations [18] (see also [19]).

In the subsequent analysis we use the slowly varying envelope approximation [20,21]. That is, we represent the solution of Eqs. (1)–(4) in the form of relatively slowly varying envelopes e_1^+, e_2^+, $\tilde{A}$, $\tilde{B}$, and rapidly oscillating components with frequencies ω_1 and ω_2 with corresponding wave-vectors k_1 and k_2

$$E_1^+ = e_1^+(z,\ t)\exp(-i\omega_1 t + ik_1 z),$$

$$E_2^+ = e_2^+(z,\ t)\exp(-i\omega_2 t + ik_2 z),$$

$$A = \tilde{A}(z,\ t)\exp(-i\omega_1 t + ik_1 z),$$

$$B = \hat{B}(z,\ t)\exp[-i(\omega_1+\omega_2)t + i(k_1+k_2)z]. \tag{5}$$

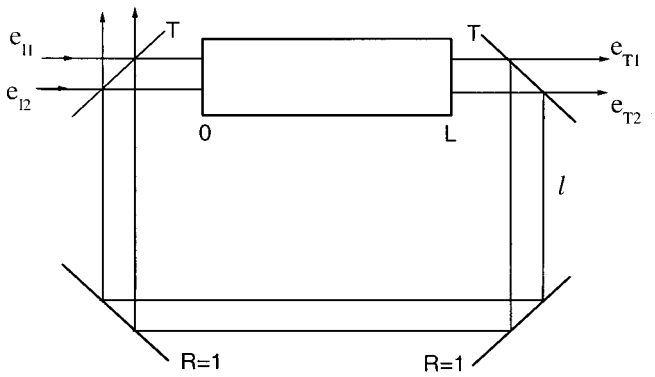

FIG. 1. A schematic diagram of the nonlinear ring cavity, $e_{I,j}$ and $e_{T,j}$ are incident and transmitted fields, respectively ($j=1,2$).

We describe the phenomenon of excitability of excitons and biexcitons in the ring cavity shown schematically in Fig. 1. The input and output mirrors have reflectivity $R=1-T$ and are separated by distance L. The other corner mirrors in the ring have a reflectivity of unity. The boundary conditions for the ring cavity are

$$e_{T,j}(t) = \sqrt{T} e_j^+(L,\ t),$$

$$e_j^+(0,\ t) = \sqrt{T} e_{I,j} + \mathrm{Re}^{i\beta_0} e_j^+(L,\ t - \Delta t), \tag{6}$$

where $\Delta t = (L_r - L)/c$ is the retardation time introduced by the feedback, $L_r = 2(L+l)$ is the length of ring cavity, c is the velocity of light in vacuum, β_0 is the cavity-laser phase detuning.

For integration of Eqs. (1) and (2) we use the mean-field theory [22,23] which corresponds mathematically to the replacement of $\int E(z)dz$ by $[E(L)-E(0)]L$. In this approximation with the trial solutions (5) and boundary condition (6), Eqs. (1)–(4) become in dimensionless form

$$\frac{dX_1}{d\tau} = \sigma_1(-X_1 + 2C_1 U + Y_1), \tag{7}$$

$$\frac{dX_2}{d\tau} = \sigma_2(-X_2 - 2C_2 UV + Y_2), \tag{8}$$

$$\frac{dU}{d\tau} = -dU - d(X_1 + X_2 V), \tag{9}$$

$$\frac{dV}{d\tau} = -V + X_2 U, \tag{10}$$

where $Y_J = e_{I,j} gG/\sqrt{T\gamma_{ex}\gamma_{biex}}$ and $X_J = e_{T,j} gG/\sqrt{T\gamma_{ex}\gamma_{biex}} = e_j^+(L,\ t) gG/\sqrt{\gamma_{ex}\gamma_{biex}}$ are the normalized field amplitudes, while $U = i\tilde{A}\sqrt{\gamma_{biex}}/\sqrt{\gamma_{ex}}G$ and $V = \tilde{B}/G$ are the normalized exciton and biexciton amplitudes, respectively. Here we have used the dimensionless time $\tau = t\gamma_{biex}$ (for a typical value of $\gamma_{biex} = 10^{12}\ \mathrm{s}^{-1}$, $\tau = 1$ corresponds to a time of 1 ps) and the following notation: $d = \gamma_{ex}/\gamma_{biex}$ is the decay rate of an exciton relative to that of a biexciton, $\sigma_j = c_j T/\gamma_{biex} L$ is the damping of the electric-field amplitude in the cavity and

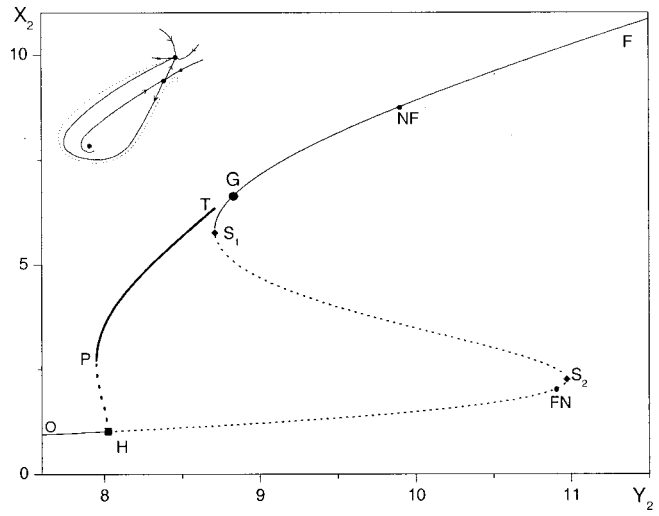

FIG. 2. The bifurcation diagram for $Y_1=10$, $\sigma=0.1$, $C_1=C_2=5$, and $d=0.1$. Thin solid: stable stationary states. Thin dotted: unstable stationary states. Thick solid: stable periodic solutions. Thick dotted: unstable periodic solutions. The square denotes a Hopf bifurcation. The rhombuses mark saddle-node bifurcations. *FN* shows the transition from unstable focus to unstable node, and *NF* the transition from stable node to stable focus. Point *G* marks the operating point. The inset: sketch of phase portrait for region $Y_2(S_1)-Y_2(S_2)$ in the plane X_2-X_1.

$C_j=\alpha_j L/4T$ with $\alpha_j=4\pi\hbar g^2\omega_j/\gamma_{\rm ex}c_j$. Close to a cavity resonance $e^{i\beta_0}\approx 1+i\beta_0$ and we consider only the real part of amplitudes.

Equations (7)–(10) completely describe the evolution of excitons and biexcitons in the ring cavity in the model used, and are the basis of the analysis that follows.

B. Bifurcation diagrams

In this section, we discuss the ring cavity dynamics of excitons and biexcitons in terms of bifurcation diagrams. The calculations were carried out with the software package AUTO97 [24] for continuation and bifurcation problems in ordinary differential equations. Specifically, we applied a numerical bifurcation analysis to Eqs. (7)–(10). The initial conditions $(X_1;\ X_2;\ U;\ V)=[Y_1/(1+2C_1);\ 0;\ X_1;\ 0]$ have been used, which correspond to the steady state with a constant pump so that there is a steady-state population of excitons. In particular, we consider the bifurcation diagram in the plane X_2-Y_2 (output amplitude-input amplitude) with the amplitude of the input pulse Y_2 as the parameter to be varied (branching parameter). Figure 2 shows a typical example of the bifurcation diagram for the system. The parameters used are $\sigma_1=\sigma_2=\sigma=0.1$, $C_1=C_2=5$, $d=0.1$, and $Y_1=10$. A thin continuous line represents stable stationary solutions, and unstable stationary solutions are indicated by a thin dotted line. A thick solid line represent a stable periodic solution. The unstable periodic solutions are marked by thick dotted line. It is well known that a Hopf bifurcation point (marked by the square) connects the stationary solution with the periodic solution. It is apparent in Fig. 2 that the periodic branch turns back and loses stability. This kind of bifurcation is described as subcritical. When Y_2 is increased from $Y_3(0)$ to $Y_2(H)$, X_2 jumps to a large amplitude periodic orbit as hard generation of a limit cycle occurs. When Y_2 is reduced from $Y_2(T)$ a discontinuity occurs again at $Y_2(P)$ with a jump from a large value to equilibrium. In the region *OP* at any given Y_2, there is only one equilibrium state, a stable focus which attracts all orbits. A stable periodic orbit, a stable equilibrium, and an unstable periodic orbit coexist in the domain $Y_2(P)-Y_2(H)$. In this interval we have a hysteresis loop of periodic solutions. Moving from *H* to *T*, a stable limit cycle is the only attractor. The periodic branch ends at *T* where a homoclinic orbit is present and the periods of periodic orbits tends to ∞. The nature of self-pulsations in the region *HT* for different parameters has been discussed in [14].

Two saddle-point bifurcations are marked by rhombuses in Fig. 2. A stability analysis of Eqs. (7)–(10) shows that between *H* and S_2 there is a transition from an unstable focus to an unstable node at point *FN*. On the other hand, at point *NF* we detect the transition from a stable node to a stable focus.

Now we discuss in more detail the region between the saddle-node bifurcations S_1 and S_2. It is known that the existence of a saddle point close to an attractor is the requirement for excitable behavior. The inset in Fig. 2 shows a sketch of the phase portraits in the plane X_2-X_1 in this region. There is an attractor (stable node in nonlinear case), a saddle, and an unstable focus for a fixed value of amplitude of the input pulse Y_2. A sufficiently large perturbation can bring the system below the stable manifold (separatrix) of the saddle point so that the system makes a big loop around the unstable focus (dotted line in inset of Fig. 2). In this region the system shows excitability with a mechanism similar to that in Ref. [6].

III. EXCITABILITY

A. Demonstration of excitability and discussion

A system is excitable if it exhibit the following properties [6,7]:

(i) the existence of a threshold above which an excitation can occur,

(ii) above threshold the form of the response independent of the perturbation magnitude,

(iii) a refractory period exists.

As noted in the previous section, our system is excitable in the region S_1-S_2, and we now discuss the dynamics of this phenomenon in more detail. We choose suitable values of the parameters to achieve excitability. The criterion for the existence of hysteresis of stationary solutions is the inequality $Y_1>\sqrt{2(1+2C_1)^2/C_2}$ [14]. The parameters σ and d influence the dynamics of the system and we choose $d=0.1$ since we consider the relaxation time of excitons to be one-order smaller than that of biexcitons. In this case for any $\sigma<0.1$ the behavior of the system is similar to that sketched in Fig. 2. We choose the operating point close to the saddle-point S_1. First we consider the response of the system to a

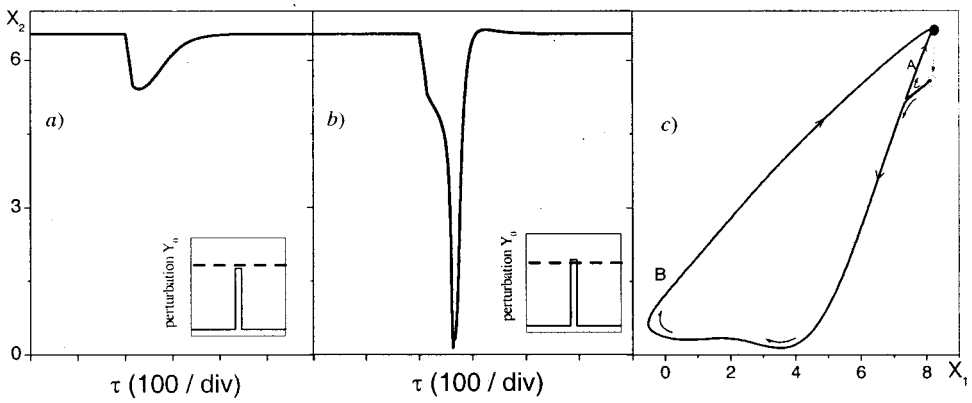

FIG. 3. Transient response to a rectangular input perturbation for $Y_2=8.8$ and initial condition which correspond to point G in Fig. 2. The perturbation amplitudes are (a) $Y_0=0.69$ and (b) $Y_0=0.70$. (c) Trajectories in the phase plane X_2-X_1; trajectory A corresponds to a subthreshold and trajectory B to a superthreshold stimulus. The parameters are as in Fig. 2.

rectangular input pulse of amplitude Y_0. The initial conditions correspond to point G in Fig. 2, for which $Y_2=8.8$. For this point we found the threshold perturbation value $Y_0=0.695$. Figure 3(a) shows the response of the system to a perturbation of amplitude $Y_0=0.69$, which is below threshold. When the amplitude of the perturbation is increased to $Y_0=0.7$ which is above the threshold the system starts to exhibit excitable behavior with a significant pulselike reduction in X_2 as shown in Fig. 3(b). To study the trend of trajectories in the phase space, let us assume that the duration $\delta\tau$ of applied stimulus Y_0 is much shorter than the characteristic time of the system. In that case the stimulus affects only the amplitude X_2 and the phase trajectories start at $(X_1, X_2, U, V)=(X_1^{\rm st}, \delta X_2, A^{\rm st}, B^{\rm st})$. Figure 3(b) shows the trajectories in the plane X_2-X_1, for a stimulus below threshold-trajectory A ($\delta X_2=1.05$), and above threshold-trajectory $B(\delta X_2=1.06)$. Trajectory A turns back to equilibrium in contrast to trajectory B which makes a big loop around the unstable focus. The position of trajectory A is situated higher than the stable manifold of the saddle (see inset of Fig. 2) while the starting point of trajectory B is down that stable manifold. The threshold is situated along the stable manifold. The dependence of excitable threshold $X_2^{\rm th}$ on Y_2 is shown in the inset of Fig. 4. With the increase of Y_2 from $Y_2(S_1)$, the saddle point moves down and the amplitude of threshold increases meaning that the system becomes less excitable. Figure 4 shows the dependence of the value of the minimum in the response of the transmitted field $X_2^{\rm min}$ on the amplitude of the perturbation Y_0 for two different values of Y_2. It shows that near S_1 we need only a small perturbation amplitude in contrast to point S_2, where a higher-perturbation amplitude is necessary to achieve excitability and also the jump at the threshold is less pronounced. However above threshold the response is essentially independent of perturbation magnitude, and the second characteristic of excitability is fulfilled.

Finally we give an example to confirm the existence of a refractory period. Two pulses with amplitudes above threshold are applied to the system. Figure 5(a) shows the response of the system when the delay time between pulses is $\tau_d=25$. It does not differ from the response to a single pulse (see Fig. 3(b) for comparison). When the second pulse is applied with delay time $\tau_d=50$ there is a small reaction to it. After increasing τ_d further to 75 we can distinguish a clear response to the second pulse. The system is able to make a distinct and essentially identical response to both pulses when $\tau_d>100$. We conclude that for this set of parameters the refractory time is the order of 45τ.

B. Applications of excitability

One motivation for research into excitability is its possible application in all-optical signal processing. This section shows some examples of the possible applications of excitability. As an optical limiter, the excitable element could serve to limit or suppress the noise level and any pulses below threshold. The excitable element can also be used as a logic element. For a subthreshold input we have zero output, but for an input above threshold the output is a one signal.

Consider a sequences of pulses ($\tau=15$ width) with different amplitudes and different delay time between pulses, such as the case shown in Fig. 6(a). We observe a big response only to input pulses which exceed the threshold. Other pulses cause negligible response and should be recognized as zero

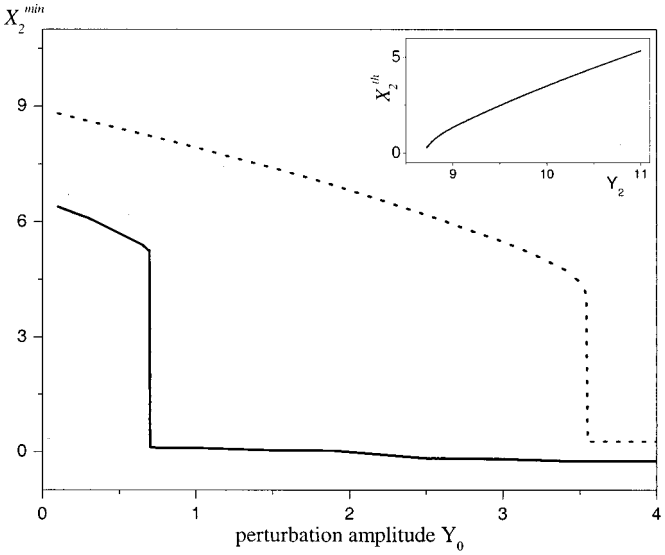

FIG. 4. The dependence of the value of the minimum in the response of the amplitude of transmitted field $X_2^{\rm min}$ on the amplitude of perturbation Y_0 for $Y_2=8.8$ (solid line) and for $Y_2=10$ (dotted line). The inset shows the dependence of excitability threshold $X_2^{\rm th}$ on injected amplitude Y_2 in the excitable region $Y_2(S_1)-Y_2(S_2)$. The other parameters are $Y_1=10$, $\sigma=0.1$, $C_1=C_2=5$, and $d=0.1$.

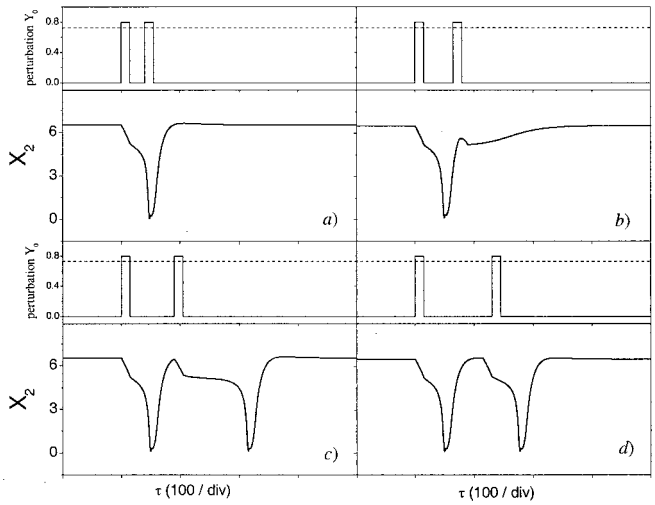

FIG. 5. Response of the system to two consecutive input pulses with amplitude above threshold ($Y_0=0.8$) and different delay time τ_d between pulses (a) $\tau_d=25$, (b) $\tau_d=50$, (c) $\tau_d=75$, and (d) $\tau_d=125$ ($\tau_d=\gamma_{\mathrm{biex}}t$). The other parameters are $Y_1=10$, $\sigma_1=\sigma_2=0.1$, $C_1=C_2=5$, $d=0.1$, and $Y_2=8.8$.

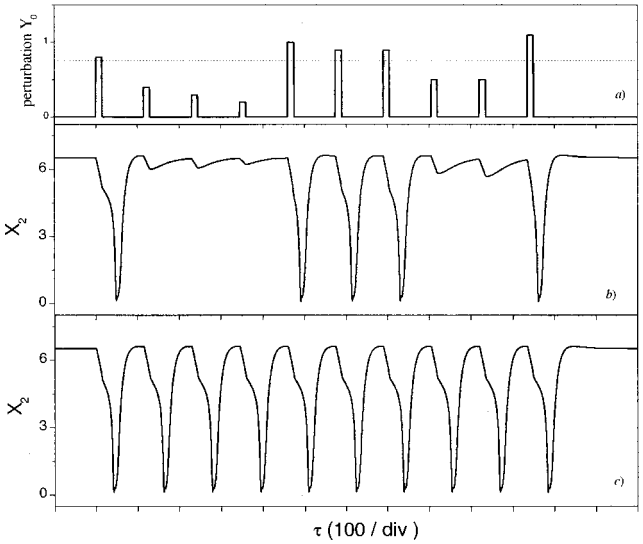

FIG. 6. (a) An input sequence of pulses with different amplitudes, (b) response X_2 to the pulses in (a), (c) response of the system to a sequence of equally spaced pulses above threshold. The other parameters are $Y_2=8.8$, $Y_1=10$, $\sigma=0.1$, $C_1=C_2=5$, and $d=0.1$.

signals. The dashed line indicates the threshold of the pulse amplitude. The selection criterion (position of threshold) can be varied by changing the parameters of the system. When all the pulses exceed the threshold, the response is similar to coherent resonance. Figure 6(c) shows such a response to above threshold, equally spaced pulses at a value of $\tau=50$.

Hitherto it has been tacitly assumed that the experimental detection of excitability may be realized for a system of excitons and biexcitons in a ring cavity. Here we consider whether it is possible to choose the parameters for CuCl crystal so that the operating point is in the excitable region. For CuCl reasonable material parameter values are: binding energy of biexcitons is 40 meV, $\gamma_{\mathrm{ex}}=0.03$ meV, $\gamma_{\mathrm{biex}}=0.3$ meV, $\hbar g=0.3$ eV/(cm$^{1/2}$ V), $G=1.25\times10^{8}$ cm$^{3/2}$. For a cavity with $L=3\,\mu$m and $T=0.01$, the intensities $I_1\approx|E_1|^2=10$ kW/cm^2 and $I_2\approx|E_2|^2=89$ kW/cm^2 ensure that the cavity is in the excitable region. On the basis of our investigations and parameter estimations we conclude that it should be possible to observe excitability in a system of excitons and biexcitons in a ring cavity.

IV. CONCLUSIONS

We have shown that excitability of excitons and biexcitons in a ring cavity can occur. In the bifurcation analysis it is found that the excitable region is situated in the domain where a saddle point is close to an equilibrium. In contrast to the excitable behavior of two-level atoms in ring cavity [5], where the behavior is similar to the FitzHugh-Nagumo model, excitons and biexcitons in a ring cavity show an other type of excitability, similar to that in a laser with saturable absorber [6], where a perturbation can push the system above the stable manifold of a saddle point. We have demonstrated the existence of the threshold above which the system shows a long excursion in phase space. The amplitude of the output field for a perturbation above threshold is independent of this perturbation. The presence of a refractory period has also been demonstrated. A set of cavity and material parameters have been identified for a system which could give an experiment demonstration of the kind of excitability discussed. It is concluded that the type of excitable system considered has possible applications as a functional optoelectronic element.

ACKNOWLEDGMENTS

V.T. acknowledges current financial support through a Royal Society/NATO grant and previously from the Alexander von Humboldt Foundation. V.T. expresses his gratitude for the hospitality of the Department of Physics at the University of Durham. The authors thank H.-J. Wuensche, K. Schneider, and M. Radziunas for useful comments.

[1] R. FitzHugh, Bull. Math. Biophys. **17**, 257 (1955).

[2] J. Rinzel and G. B. Ermentrout, in *Analysis of Neural Excitability and Oscillations, Methods in Neuronal Modeling*, edited by C. Koch and I. Segev (MIT, Cambridge, MA, 1989).

[3] J. D. Murray, *Mathematical Biology* (Springer, New York, 1990).

[4] S. Grill, V. S. Zykov, and S. C. Müller, J. Phys. Chem. **100**, 19 082 (1996).

[5] W. Lu, D. Yu, and R. G. Harrison, Phys. Rev. A **58(2)**, R809 (1998).

[6] L. A. Johan Dubbeldam, Bernd Krauskopf, and Daan Lenstra, Phys. Rev. E **60(6)**, 6580 (1999).

[7] J. Mullet and C. R. Mirasso, Phys. Rev. E **59**, 5400 (1999).
[8] V. Tronciu, H.-J. Wuensche, K. Schneider, and M. Radziunas, in *SPIE Proceedings, Physics, and Simulation of Optoelectronic Devices IX, Vol. 4283*, edited by Y. Arakawa, M. Osinski and P. Blood (SPIE, 2001).
[9] J. R. Tredicce, *Excitability in Nonlinear Laser Dynamics: Concepts, Mathematics, Physics and Applications International Spring School*, edited by Bernd Krauskopf and Dean Lenstra, AIP Conf. Proc. No. 548 (AIP, Melville, NY, 2000), p. 288.
[10] E. Hanamura, Solid State Commun. **12**, 951 (1973).
[11] A. A. Gogolin and E. I. Rashba, Pis'ma Zh. Exp. Teor. Fiz. **17**, 690 (1973) [JETP Lett. **17**, 478 (1973)].
[12] A. L. Ivanov, H. Haug, L. V. Keldysh, Phys. Rep. **296**, 237 (1998).
[13] V. A. Zalozh, A. H. Rotaru, and V. Z. Tronchu, Zh. Eksp. Teor. Fiz **103**, 994 (1993) [Sov. Phys. JETP **76**, 487 (1993)].
[14] V. A. Zalozh, A. H. Rotaru, and V. Z. Tronchu, Zh. Eksp. Teor. Fiz **105**, 260 (1994) [Sov. Phys. JETP **78**, 138 (1994)].
[15] V. Z. Tronciu and A. H. Rotaru, Phys. Status Solidi B **212**, 383 (1999).
[16] A. L. Ivanov, M. Hasuo, N. Nagasawa, and H. Haug, Phys. Rev. B **52**, 11 017 (1995).
[17] S. A. Moskalenko and D. W. Snoke, *Bose-Einstein Condensation of Excitons and Biexcitons and Coherent Nonlinear Optics with Excitons* (Cambridge University Press, Cambridge, 2000).
[18] S. A. Moskalenko, A. H. Rotaru, and Yu. M. Shvera, Teor. Mat. Fiz. **75**, 295 (1998).
[19] C. C. Sung, C. M. Bowden, J. W. Haus, and W. K. Chiu, Phys. Rev. A **30**, 1873 (1984).
[20] J. A. Armstrong, N. Bloembergen, J. Ducuing, and P. S. Pershan, Phys. Rev. **127**, 1918 (1962).
[21] J. A. Armstrong, S. S. Jha, N. S. Shiren, IEEE J. Quantum Electron. **6**, 123 (1970).
[22] L. A. Lugiato, in *Theory of Optical Bistability*, Progress in Optics Vol. XX1, edited by E. Wolf (North-Holland, Amsterdam, 1984).
[23] H. M. Gibbs, *Optical Bistability Controling Light with Light* (Academic, New York, 1995).
[24] E. J. Doedel, A. R. Champneys, T. F. Fairgrieve, Y. A. Kuznetsov, B. Sandstede, and X. Wang, AUTO97 continuation and bifurcation software for ordinary differential equations, 1997. Available by anonymous ftp from ftp.cs.concordia.ca directory pub/doedel/auto